5

Optical Injection-Locking of VCSELs

Ahmad Hayat, Alexandre Bacou,
Angélique Rissons and Jean-Claude Mollier
Institut Supérieur de l'Aéronautique et de l'Espace (ISAE),
Toulouse
France

1. Introduction

Since the telecommunication revolution in the early 90s, that saw massive deployment of optical fibre for high bit rate communications, coherent optical sources have made tremendous technological advances. The technological improvement has been multi dimensional; component sizes have been reduced, conversion efficiencies increased, power consumptions decreased and integrability into compact optoelectronic sub-modules improved. Semiconductor lasers, emitting in the 1.1-1.6 µm range, have been the most prominent beneficiaries of these technological advances. This progress is a result of research efforts that consistently came up with innovative solutions and components, to meet the market demand. This in-phase, demand and supply, problem and solution and consumer need and innovation cycle, has ushered us in to the present information technology era, where stable high speed data links make the backbone of almost every aspect of life, from economy to entertainment and from health sector to defence production.
By the start of twenty-first century, a new, low cost, low power consumption and miniaturized generation of lasers had started to capture its own market share. These lasers, named Vertical-Cavity Surface-Emitting Lasers (VCSELs) due to the presence of an optical cavity which is normal to the fabrication plane , have established themselves as premier optical sources in short-haul communications such as Gigabit Ethernet, in optical computing architectures and in optical sensors. While shorter wavelength VCSEL (< 1µm) fabrication technology was readily mastered, due to the ease in manipulation of AlGaAs-based materials, long wavelength VCSELs especially VCSELs emitting in the 1.3-1.5 µ range have encountered several technical challenges. There importance as low-cost coherent optical sources for the telecommunication systems is primordial, since they are compatible with the existing infrastructure.
VCSEL utilization in low-cost systems imply the application of direct modulation for high bit rate data transmission which engenders the problems of frequency chirping which increases laser linewidth and severely limits the system performance. Furthermore, relatively lower VCSEL intrinsic cut-off frequencies translated in to impossibility of achieving high bit rates. Optical injection-locking is proposed as a solution to these problems. It enhances the intrinsic component bandwidth and reduces frequency chirp considerably.

Source: Advances in Optical and Photonic Devices, Book edited by: Ki Young Kim,
ISBN 978-953-7619-76-3, pp. 352, January 2010, INTECH, Croatia, downloaded from SCIYO.COM

2. Emergence of Vertical-Cavity Lasers

2.1 Historical background and motivation

It must be noted that the Vertical-Cavity Surface-Emitting Lasers (VCSELs) or simply SELs (Surface-Emitting Lasers, as they were referred to as at that time) were not proposed to overcome the bottlenecks that had hindered the progress of FTTX systems. The lasers usually used for long-haul telecommunications have cleaved structures with edge emission. Consequently they are referred to as Edge Emitting Lasers (EELs). This structure does pose some problems, e.g. the initial probe testing of these devices is impossible before there separation into individual chips. Their monolithic integration is also limited due to finite cavity length. The cavity length implies generation of undesirable longitudinal modes and the non-monolithic fabrication process implies the impossibility of fabricating laser arrays and matrices. It was specifically in order to overcome these problems that, K. Iga, a professor at that time at Tokyo University, proposed a vertical-cavity laser in 1977.
These surface-emitting lasers provided following advantages:

- Probe-testing during the manufacturing process.
- Fabrication of a large number of devices by fully monolithic processes yielding a very low-cost chip-production.
- Very small cavity length guaranteeing longitudinal single mode operation.
- Possibility of production as arrays and matrices.
- Very low threshold currents due to ultra small cavity volume.
- Monolithic integration compatibility with other devices.
- Circular far-field pattern as compared to elliptical pattern for EELs.

A pulsed operation at 77K with a threshold current of 900mA was demonstrated in 1979 with a GaInAsP-InP vertical-cavity laser emitting at 1.3μm (Soda et al., 1979). However, more pressing issues regarding the delivery of higher bit rates using the conventional EELs meant that the research into vertical-cavity lasers progressed very slowly. Consequently VCSEL research and development stagnated through out the decade that followed its first demonstration.
Continuous Wave (CW) operation of a VCSEL was presented in 1989, by Jewell et. al, for a device emitting at 850nm (Jewell et al., 1991). This VCSEL presented two unique features as compared to the previous generation of components. It had a QW-based active region and the semiconductor DBR mirrors were grown by means of Molecular Beam Epitaxy (MBE) which replaced the dielectric mirrors previously being used. The VCSEL technology then progressed steadily over the next ten years. A 2mA threshold quantum-well device was presented in 1989 (Lee et al., 1989). In 1993 Continuous Wave (CW) operation for a VCSEL emitting at 1.3μm was demonstrated (Baba et al., 1993). A high power VCSEL emitting at 960nm and with an output of 20mW CW output was reported in 1996 (Grabherr et al., 1996).
Despite these advances and maturity in fabrication technology, the VCSELs could not replace the EELs as optical sources for long-haul telecommunications and were hence confined to other applications such as optical computing, sensors, barcode scanners and data storage etc.
The reason for this shortcoming lies in the VCSEL physical structure that gives priority to:

- Monolithic integration favouring vertical emission
- Low threshold current
- On chip testing

These priorities impose a set of design guidelines for VCSEL fabrication which, when implemented, induce certain unwanted and unforeseen traits in the device behaviour. These undesirable characteristics rendered the VCSEL unsuitable for utilization in prevalent telecommunication systems.

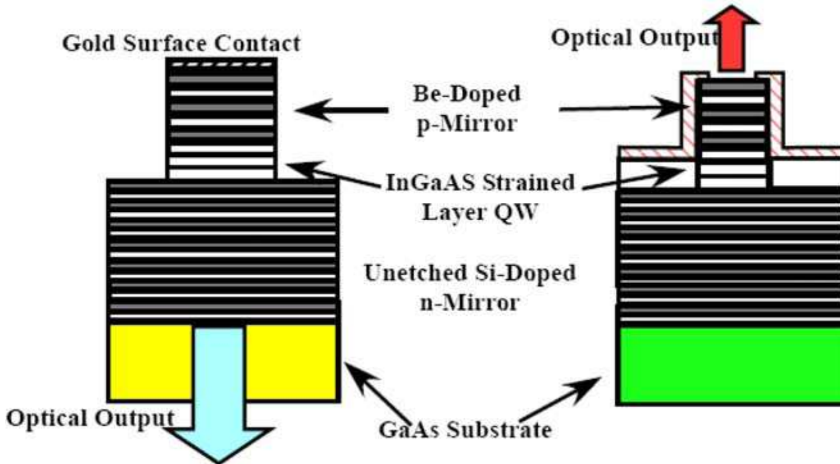

Fig. 1. An early design schematic for top-emitting and bottom-emitting VCSELs presented by Jewell et. al. in 1989.

Following is a concise analysis of these shortcomings. We would present the basic VCSEL structure that would try to achieve the above given objectives. Following this discussion we would present the drawbacks in the device performance related to the realization of design objectives. Certain remedies and improvements would then be presented in order to render the device more performing and efficient.

2.2 VCSEL structure

A VCSEL is essentially a gain medium based active region vertically stacked between two Distributed Bragg Reflectors (DBRs). In order to achieve a single mode operation it is proposed that the length of the active region be very small: Effectively of the order of the desired lasing wavelength. A short cavity eliminates the generation of longitudinal modes associated to Fabry-Pérot cavities. This however imposes a severe restriction on VCSEL DBR design.

The threshold gains for the surface-emitting and edge-emitting devices must be comparable regardless of the cavity length. The threshold gain of an EEL is approximately $100 cm^{-1}$. For a VCSEL of active layer thickness of 0.1 μm, this value corresponds to a single-pass gain of about 1%. Thus for a VCSEL to lase with a threshold current density comparable to that of an EEL, the mirror reflectivities must be greater than 99% in order to ensure that the available gain exceeds the cavity losses during a single-pass.

Achieving a reflectivity of 99% with DBRs is a formidable task and thus central to the conception of low threshold VCSELs is the capacity to fabricate high reflectivity mirrors. Let's consider the example of a VCSEL operating at 850nm. The active region would consist of several ultra thin layers composed alternately of GaAs and AlGaAs materials. The

difference between the refractive index of layers of a pair determines the number of pairs required to achieve a reflectivity of 99% or more. In the case of AlAs-$Al_{0.1}Ga_{0.9}As$ the refractive index difference between two alternate layers is 0.6 as is shown in fig. 2 (Adachi, 1985). Consequently only 12 pairs are needed to achieve a reflectivity of 99% or more. As far as AlAs and $Al_xGa_{1-x}As$ alloys go, the situation is conducive, even desirable, for the fabrication of VCSELs using these materials. The band gap energy of AlAs−$Al_xGa_{1-x}As$ alloys is about 1.5eV which eventually corresponds to a wavelength in the 800-900nm region.

Fabrication technology for VCSELs emitting in this wavelength band therefore has perfectly been mastered since monolithic growth of 12-15 DBR pairs does not pose serious fabrication challenges. Furthermore AlAs-GaAs alloy DBRs have an excellent thermal conductivity which allows the dissipation of heat fairly rapidly and avoids device heating which eventually could have been responsible for VCSEL underperformance.

2.3 Performance drawbacks

As far as the fabrication of near infrared VCSELs was concerned, the existing technologies and fabrication processes proved to be quite adequate. However, applying a similar methodology to telecommunication wavelength VCSELs proved to be much more challenging. Long wavelength VCSELs operating in the 1.1μm- 1.6μm range are of considerable interest for optical fibre telecommunications since the hydroxyl absorption and pulse dispersion nulls for silicon optical fibres are found at 1.5μm and 1.3μm respectively.

Although several material systems were considered, the combination InGaAsP-InP turned out to be the most suitable in view of the near perfect lattice match. The active layer is composed of the $In_{1-x}Ga_xAs_yP_{1-y}$ quaternary alloy. By varying mole fractions x and y, almost any wavelength within the 1.1−1.6μm can be selected.

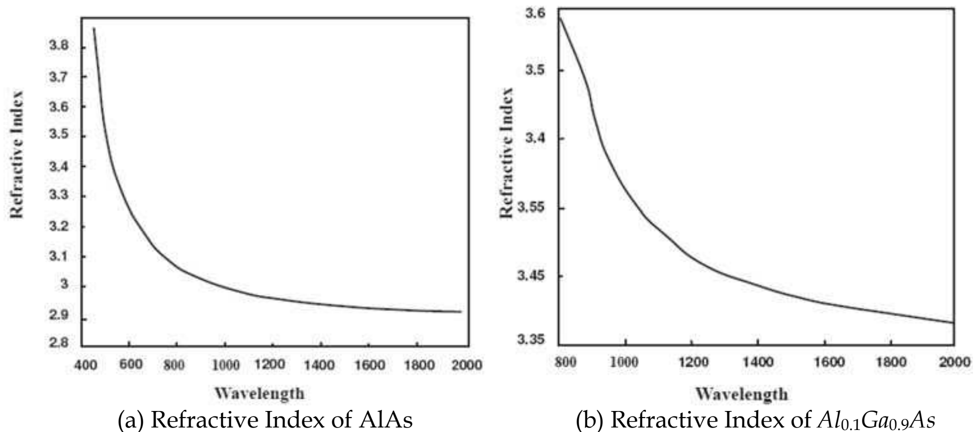

(a) Refractive Index of AlAs (b) Refractive Index of $Al_{0.1}Ga_{0.9}As$

Fig. 2. Refractive indices of AlAs and $Al_{0.1}Ga_{0.9}As$ as a function operating wavelengths.

2.4 DBR growth

Only 12−15 AlAs−$Al_xGa_{1-x}As$ pairs are needed to fabricate a DBR with a 99% reflectivity. By contrast, the refractive index difference between an InP- InGaAsP pair is only 0.3 and hence more than 40 pairs would be needed to achieve a reflectivity of 99%. The problem

consequently encountered concerns thermal properties of InP−based materials that intervene to affect the process in following ways (Shau et al., 2004), (Piprek, 2003):

- For the fabrication of long wavelength VCSELs, there are mainly $In_{1-x}Ga_xAs_yP_{1-y}$ alloys available which have to be grown on InP substrates. Due to the effects of non negligible Auger's recombination effects and intra-valence band absorption, these materials suffer from temperature-dependent losses.
- The thermal conductivity is greatly reduced due to alloy disorders which causes phonon scattering. This reduction in thermal conductivity is particularly adverse for effective heat sinking through the VCSELs' DBRs usually having a thickness of several µms.
- AlAs-$Al_xGa_{1-x}As$ DBRs have a good thermal conductivity and could be thinner but due to lattice mismatch could not be grown on the InP substrate.

DBR growth has been one of the fundamental problems regarding the fabrication of long wavelength VCSELs that has hampered the entry of VCSELs in high-speed data, command and telecommunications domain.

2.5 Optical and electrical confinement

Growing stacks of DBRs was not the only problem encountered by VCSEL manufacturers. One of the primary objectives of VCSEL design was to fabricate short cavity single mode devices. The short cavity did eliminate the undesirable longitudinal modes but it gave birth to another unforeseen problem. Initial VCSEL designs suggested that the carriers and the photons share a common path traversing the DBRs. This led to the heating of certain zones of the DBRs due to carrier flow and resulted in a variable refractive index distribution inside the VCSEL optical cavity. This phenomenon is known as "Thermal Lensing". Instead of being concentrated in the centre in the form of a single transverse mode, the optical energy is repartitioned azimuthally inside the optical cavity. This particular optical energy distribution is observed in the form of transverse modes. Higher bias currents therefore imply high optical power and in consequence a higher number of transverse modes.

An oxide-aperture is employed, principally in shorter wavelength emission VCSELs, in order to block the unwanted transverse modes. The oxide-aperture diameter then determines the multimode or single mode character of a VCSEL. VCSELs having oxide aperture diameter greater than 5µm exhibit multimode behaviour. It can also be inferred from the above discussion that for the type of VCSELs employing the oxide-aperture technology for optical confinement, single mode VCSELs almost always have emission powers less than those of multimode VCSELs.

The problems of optical and electrical confinement are hence interrelated. It is evident that in order to attain single mode emission the thermal lens effect must be avoided. This can only be achieved by segregating the carrier and photon paths. Although challenging technically, it can be achieved using a tunnel junction. The concept and functioning of a tunnel junction is explained in the following sub-section.

2.6 The tunnel junction

The "Tunnel Junction" was discovered by L. Esaki in 1951 (Esaki, 1974) and the tunnel junction diodes used to be labeled "Esaki Diodes" for quite some time after this discovery (Batdorf et al., 1960), (Burrus, 1962). Esaki observed the tunnel junction functioning while working on Ge layers but soon after his discovery, tunnel junction diodes were presented by

other researchers on other semiconductor materials such as GaAs, InSb, Si and InP. The tunnel junction is formed by joining two highly doped (degenerate) “p” and “n” layers. It has a particular current-voltage characteristic curve. A negative differential resistance region ($-$ dI/dV) over part of the forward characteristics can be observed.
In the case of a VCSEL the tunnel junction serves a “Hole Generator”. Under the tunnel effect, the electrons move from valence band (doped p++) to conduction band (doped n++), leaving holes in their place. Fig.1.12 shows the schematic diagram of a tunnel diode in reverse bias conditions. The existence of a tunnel junction in a VCSEL presents following advantages:
- It reduces the intra valence band absorption due to P doping.
- It serves to reduce the threshold current, by improving the carrier mobility.
- It is used for electrical as well as optical confinement.

Due to these properties, the tunnel junction has become an integral part of long wavelength VCSELs.

2.7 Technological breakthroughs and advances in long wavelength VCSEL fabrication

Although by the start of the 21st century serial production and delivery of VCSELs was in full flow for diverse applications, they had failed to fulfil the two following essential criteria for utilization in optical networks.
- They did not emit in the 1.3µm and 1.5µm range: The so-called “Telecoms Wavelengths”. This meant not only definition and standardization of new standards at 850nm wavelength but also the deployment and manufacturing of a host of optical components such as optical fibres, couplers, multiplexers and photodiodes compatible with the 850nm emission range.
- As has been explained above, transverse-mode operation starts to manifest itself from a few milli-amperes above the threshold current rendering the VCSELs multimode in character. This multimodality is disconcerting in two ways:
  - It reduces the effective channel bandwidth hence reducing the maximum deliverable bit rate.
  - It requires the utilization of multimode optical fibre which although being less expensive than the single mode fibre, affects the VCSEL operation in another way. When high optical powers are injected in a multimode fibre, several undesired fibre modes are excited thus reducing the effective bandwidth.

It is clear from the above discussion that a suitable substitute for EELs, for applications in short to medium distance optical fibre networks, must possess the following properties:
- It must emit at either 1.3µm or at 1.5µm wavelength so that the existing standards, infrastructure, optoelectronic components and devices could be utilized.
- It must have a single mode emission spectrum so as to profit from the high bandwidths offered by the employment of single mode optical fibres.

As late as 2000, there were no serial production and mass deployment of VCSELs that fulfilled these two essential criteria. As has been discussed above, this was due to the technical challenges posed by a combination of several different factors which rendered the fabrication of long wavelength VCSEL devices very difficult.

2.8 Emergence of long wavelength VCSELs

Regarding the manufacturing of long wavelength VCSELs, several different research groups kept trying to realize long wavelength emission devices. In 1993, Iga et al. demonstrated the

CW operation of a 1.3μm InGaAs-InP based VCSEL at 77K (Soda, 1979). The upper DBR consisted of 8.5 pairs of p-doped MgO-Si material with Au-Ni- Au layers at the top while the bottom DBR consisted of 6 pairs of n-doped SiO-Si material (Dielectric Mirror). In 1997, Salet et.al demonstrated the pulsed room-temperature operation of a single mode InGaAs-InP VCSEL emitting at 1277nm. The bottom mirror consisted of n-doped InGaAsP-InP material grown epitaxially to form a 50 pair DBR mirror with a 99.5% reflectivity (Salet et al., 1997).

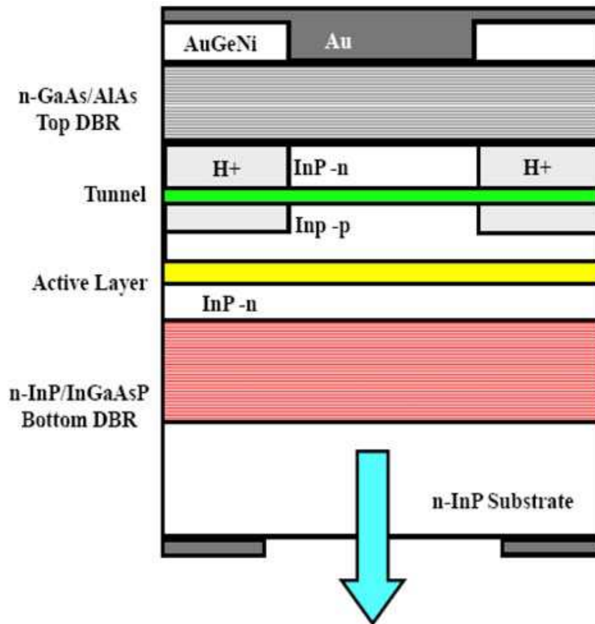

Fig. 3. A long wavelength VCSEL with a tunnel junction emitting at 1.55μm presented by Boucart et. al in 1999.

The device threshold current at 300K was 500mA. The top mirror was realized using p-doped SiO_2-Si reflectors. A year later, in 1998, Dias et al. reported the growth of InGaAsP-InP, AlGaInAs-AlInAs and AlGaAsSb-AlAsSb based DBRs on InP substrates to achieve reflectivities up to 99.5% (Dias et al., 1998). Soon afterward, in 1999, Boucart et al extended their previous work to demonstrate the room temperature CW operation of a 1.55μm VCSEL. In this case the top DBRs consist of 26.5 n-doped GaAs-AlAs pairs which were grown directly on an n-InP substrate (Metamorphic mirrors). A tunnel junction was fabricated to localize the current injection. The bottom mirror consisted of 50 pairs of n-doped InGaAsP-InP layers having a reflectivity of 99.7%. The device had a threshold current of only 11mA and had been fabricated using gas-based Molecular Beam Epitaxy (MBE) (Boucart et al., 1999).
The tunnel junction proved benificial in two ways:

- It enabled the utilization of two n-doped DBRs;
- Once the conductive properties of the tunnel junction were neutralized using H+ ion implantation, it served to localize the current injection without having to etch a mesa.

The resulting device was therefore coplanar in structure. It can be ascertained from Table.1.1 that several different materials such as InGaAsP, InGaAsAl, InGaAsSb and InGaAsN were chosen to fabricate the active layer. The material choice for DBRs and the fabrication processes were equally diverse. Although most of the research groups chose "Monolithic Integration Techniques" for the fabrication of VCSELs, "Wafer Fusion", and "Fusion Bonding" were also applied.
Meanwhile, in 1998, the Institute of Electrical and Electronics Engineers (IEEE) defined the "1000BASEX-Gbps Ethernet over Fibre-Optic at 1Gbit/s" standard. This standard for the transmission of "Ethernet Frames" at a rate of at least one Gbps was defined using light sources emitting at 850nm. The definition of Gigabit Ethernet standards using 850nm optical sources boosted the research and development of near infrared emission VCSELs. By the year 2000, 850nm VCSELs had firmly established themselves as standard optical sources for short-haul communication applications. This development was a setback for ongoing research in long wavelength VCSELs and as a result many research groups shifted their focus from long wavelength VCSEL development to other emerging fields. Furthermore, the research focus, even in the long wavelength VCSEL development field, shifted toward a new dimension. Long wavelength VCSELs were no longer being developed solely as telecommunication sources, an emerging field of spectroscopy was beginning to play an increasingly important part in eventual long wavelength VCSEL applications.

2.9 Vertilas VCSELs

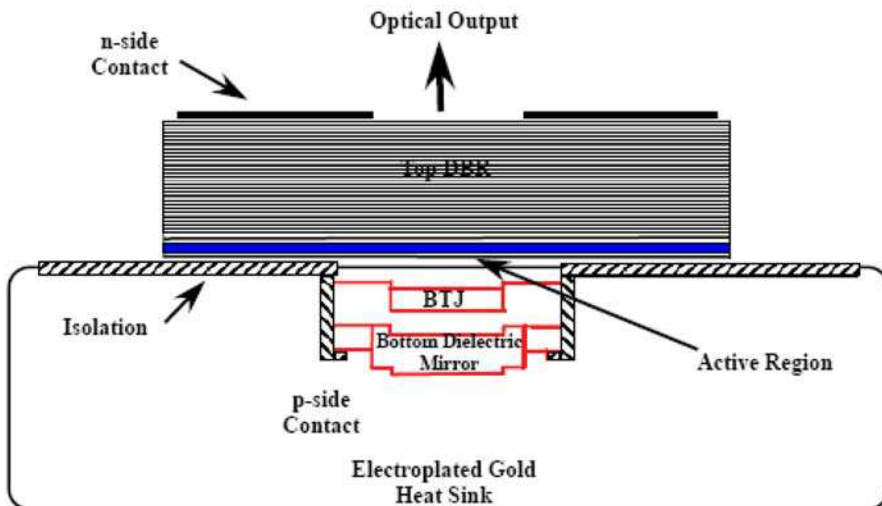

Fig. 4. A Vertilas BTJ structure with an emission wavelength of 1.55μm [28].

Although long wavelength VCSEL operation using a tunnel junction device was already demonstrated by Boucart et al. in 1999, Ortsiefer et al. presented a variation to this concept. Soon the single mode room temperature operation of an InP-based VCSEL operating at 1.5μm was demonstrated by the same research group (Ortsiefer et al., 1999), (Ortsiefer et al., 2000). The top DBR is composed of 34.5 InGaAlAs-InAlAs pairs. The bottom mirror is comprised of 2.5 pairs of CaF2-Si with Au-coating. The gold coating, apart from serving as a

high reflectivity mirror (99.75%), serves as an integrated heat sink (Shau et al., 2004). The successful incorporation of tunnel junction in the long wavelength VCSEL design proved to be the technical breakthrough that would present VCSELs as standard devices for short to medium distance optical fibre communications. By 2002 Vertilas was delivering 1.55μm single mode VCSELs for 10Gbps operation.

2.10 BeamExpress VCSELs

The manufacturing of a long wavelength VCSEL requires the growth of an InP-InGaAsP alloy active region on an InP substrate. These alloys however are difficult to grow as DBR stacks above and below the active region since the restrictions imposed by the material thermal conductivity render proper device functioning impossible. On the other hand, AlAs-$Al_xGa_{1-x}As$ DBRs have a good thermal conductivity but they can not be monolithically grown on InP-based substrates due to lattice mismatch. The solution to the matching of disparate materials to optimize VCSEL performance was developed at the University of California Santa Barbara (UCSB) in 1996 by Margalit et al. (Margalit et al., 1996). The technique utilized is known as “Wafer Fusion” or “Wafer Bonding” and consists of establishing chemical bonds directly between two materials at their hetero-interface in the absence of an intermediate layer (Black et al., 1997). The first demonstration constituted of fabrication of a 1.55μm VCSEL. The device was fabricated by wafer fusion of MOVPE-grown InGaAsP quantum well active region to two MBEgrown AlGaAs-GaAs DBR reflectors (Margalit et al., 1996).

By applying a variant of the “Wafer Fusion” technique in 2004, Kapon et. al demonstrated that it was possible to grow separate components of a VCSEL cavity on separate host substrates (Syrbu et. al, 2004), (Syrbu et. al, 2005). These separate components were then bonded (fused) together to construct the complete VCSEL optical cavity. This process was developed at the Ecole Polytechnique Fédérale de Lausanne (EPFL) and patented as “Localized Wafer Fusion”. Fig. 5 presents the structure of a BeamExpress VCSEL with an emission wavelength of 1.55μm. This is a double intracavity contact single-mode VCSEL with coplanar access. The InP-based optical cavity consists of five InAlGaAs quantum wells. The top and bottom DBRs comprise of 21 and 35 pairs respectively and are grown by Metal-Organic Chemical Vapor Deposition (MOCVD) epitaxy method. Using the technique of localized wafer fusion, the top and the bottom AlGaAs-GaAs DBRs are then bonded to the active cavity wafer and the tunnel junction mesa structures. Using VCSELs with double intracavity contacts has its own advantages. These contacts are much nearer to the active region than the classical contacts. Their utilization combined with the presence of tunnel junction allows having lower series resistance as compared to oxidized-aperture VCSELs. Due to this proximity of the contacts to the active region these VCSELs tend to have high quantum efficiency. Their location near the active region results in no current passage through DBRs.

The process used for the fabrication of Beam Express VCSELs is not monolithic. The bottom AlGaAs-GaAs DBR is grown on the GaAs substrate. The InP-based cavity is then bonded to this DBR. After the growth of an isolation layer on the active region, the epitaxially grown AlGaAs-GaAs top DBR is fused to complete the optical cavity. This double fusion increases the complexity of the fabrication process but it presents certain advantages. Waferfusion allows replacing the InAlGaAs DBRs by GaAs DBRs. Not only the GaAs DBRs have a better thermal conductivity, they are much cheaper than InAlGaAs DBRs which allows increasing the performance and decreasing the cost of the component at the same time. The biggest

advantage of "Wafer Fusion" is the possibility of serial production of VCSELs which further serves to reduce the component cost.

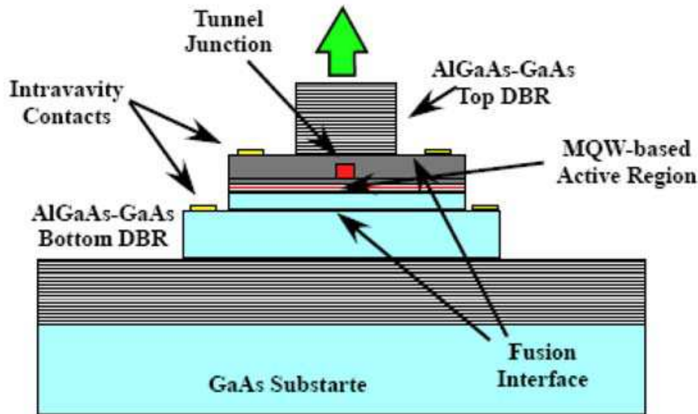

Fig. 5. Schematic diagram of a wafer-fused Beam-Express VCSEL with an emission wavelength of 1.5µm.

2.11 RayCan VCSELs

Starting as a spin-off company from the Korean government funded Electronics and Telecommunications Research Institute (ETRI) in 2002, RayCan launched an ambitious project for manufacturing of long wavelength VCSELs. Instead of using the above described specialized technologies for long wavelength VCSEL manufacturing, RayCan decided to embark upon a different course. They decided to monolithically grow InAlGaAs DBRs and an InGaAs-based quantum well active region on an InP substrate. As has been discussed above, this technique was previously not considered because in order to achieve 99% reflectivity using InAlGaAsbased DBRs, a growth of more than 40 pairs is needed. RayCan employed Metal-Organic Chemical Vapour Deposition (MOCVD) technique to fabricate a long wavelength VCSEL.

For 1.55µm VCSELs, the top and bottom DBRs were grown as 28 and 38 pairs of un-doped InAlGaAs-InAlAs schemes. The top and bottom DBRs consisted of 33 and 50 layers respectively for 1.3µm emission VCSELs. The 0.5λ thick active region consists of seven pairs of strain-compensated (SC) InAlGaAs quantum wells (Park et al., 2006). The lower number of top DBRs in both the VCSELs was compensated by using an InAlGaAs phasematching layer and Au metal layer. Fig. 6 presents the structure of a RayCan VCSEL emitting at 1.5µm. RayCan has been shipping 1.3µm and 1.5µm VCSELs since 2004. In November 2005 RayCan shipped its first 10GBit/s long wavelength CWDM VCSEL module.

2.12 Long wavelength VCSEL direct modulation

Up to this point we have discussed the prospects of long wavelength VCSELs in the context of high bit rate data delivery over medium and short distance links. It would not be an exaggeration to state that consumer demand for multimedia and interactive applications and therefore bandwidth has increased to an unprecedented level. Current electrical-electrical infrastructures can not support this demand. The major obstacle in switching from

electrical/ hertzian systems to optical/fibred systems is the cost of the coherent optical source compatible with existing infrastructure. Recent advances in the fabrication, development and serial production of VCSELs emitting at 1.3μm and 1.5μm have paved the way for future FTTX systems.

Having been able to solve the problem at component level, by developing reliable long wavelength VCSELs, the next logical approach is the development of new systems incorporating these components. Conventionally the EELs used in the long-haul fibre links are externally modulated i.e. the photon generation process inside the cavity is independent of the modulation mechanism. While being extremely effective, this method necessitates the utilization of an external modulator which increases the system cost. Such a scheme is inherently unfeasible for FTTX systems due to the cost of the external modulators. The elimination of external modulators as a component of choice for FTTX systems decrees the employment of direct modulation techniques. In this technique the laser diode bias current is varied to achieve the optical output intensity variation. Apparently the scheme is simple and easy to implement, but when put into practice, it presents two major problems which are detailed in the following two sub-sections.

2.13 Phase-amplitude coupling

Semiconductor lasers, whether EELs or VCSELs, are different from other lasers in one respect. The refractive index of a semiconductor laser depends on the carrier concentration inside the cavity. The carrier concentration variation affects the refractive index of the cavity which eventually changes the emission wavelength of the component. The consequences of this uniqueness manifest themselves during the process of direct modulation. A variation in bias currents varies the optical output power as well as the optical frequency of the cavity. These variations are proportional to the variation in carrier concentration and therefore the bias current.

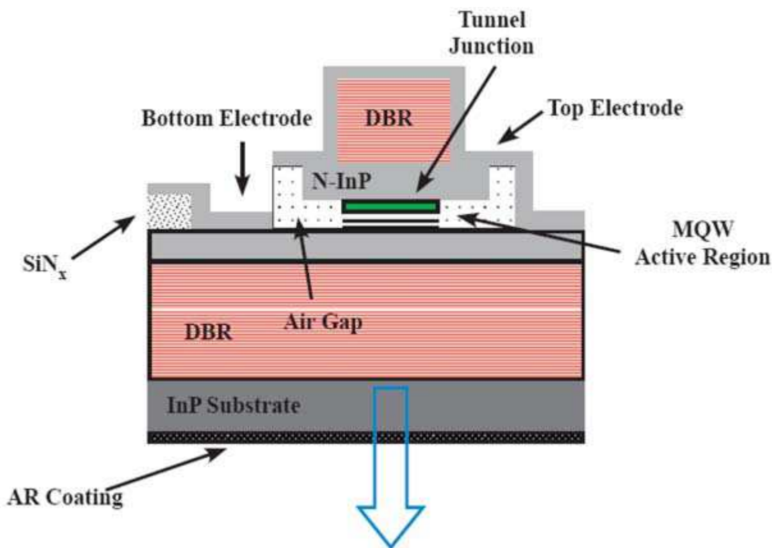

Fig. 6. MOVCD Grown monolithic structure of a 1.5μm RayCan VCSEL.

The device is modulated in amplitude and frequency at the same time. This phenomenon of "Phase-Amplitude Coupling" or the dynamic shift of the lasing frequency during modulation is known as "Frequency Chirping" or simply "Chirping".
Chirping broadens the linewidth of a laser. The extent to which a pulse broadens depends upon the amplitude of the modulating signal. Larger modulation amplitudes result in linewidths of the order of GHz 1. This spectral broadening at the time of modulation becomes more pronounced during the passage of the modulated pulse through an optical channel and the effective channel bandwidth is reduced. Direct modulation while being costeffective proves to be inefficient, in terms of deliverable bit rates, when compared to external modulation.

2.14 Intrinsic modulation limits

A semiconductor optical cavity, in essence, is a resonator. Like every resonator, or electrical circuit for that matter, its frequency response depends on its intrinsic parameters. In case of semiconductor lasers these parameters might be cavity volume, photon and electron populations, group velocity, gain compression factor etc. When directly modulated, a laser can not better the modulation frequency response already defined by these intrinsic parameters. On the other hand, the utilization of an external modulator provides a means to bypass the laser intrinsic parameters. The modulation response (or the deliverable bit rate) of the system is then defined by the external modulator and not the laser.

2.15 Long wavelength VCSEL optical injection-locking

It is clear from the description of the two above given problems that a viable optical system must minimize the effects of "Amplitude-Phase Coupling" and "Intrinsic Modulation Limits" in order to be efficient and acceptable. Once injection-locked, the master laser holds the frequency of the follower laser and makes it immune to carrier variations. This isolation from carrier variations appears as the reduction of chirp during direct modulation. In 1984, Lin et al. demonstrated the reduction of frequency chirping in a directly modulated semiconductor laser by the application of injection-locking technique (Lin et al., 1984).
Henry presented an approximate formula for the calculation of resonance frequency of optically injection-locked semiconductor lasers (Henry et al., 1985) but its significance was not appreciated at that time until Simpson and Meng demonstrated bandwidth and resonance frequency enhancements in late 90's (Simpson et al., 1996), (Meng et al., 1998). In 2002, a research group in University of California Berkley (UCB), led by Connie J. Chang-Hasnain reported the first optical injection-locking of a long wavelength VCSEL for 2.5Gbps transmission (Chang et al., 2002).
In 2003 long wavelength VCSEL chirp reduction and bandwidth enhancement were presented by the same research group (Chang et al., 2003) but there was a marked technical difference from their first publication. Whereas the first time optical injection-locking of a long wavelength VCSEL was carried-out using an identical VCSEL, the second demonstration used a Distributed FeedBack (DFB) laser to injection-lock a long wavelength VCSEL. The group has extensively published on the subject of the optical injection-locking of long wavelength VCSELs, but this pattern of locking a VCSEL with a DFB has remained unchanged since.
Several optical injection-locking studies regarding semiconductor lasers have reported frequency-chirp reduction (Lin et al., 1984), (Sung et al., 2004) increased RF link gain

(Chrostowski et al. 2003), (Chrostowski et al. 2007), improved relative intensity noise (Yabre et al., 2000) and diminished non-linear distortion (Chrostowski et al. 2007). Although the utilization of a DFB laser to injection-lock a VCSEL is excellent for demonstration of phenomena related to optical injection-locking, its practical application presents two major drawbacks. Without immediately entering into the details of these drawbacks, it can be logically inferred that both these drawbacks are related to the utilization of the DFB laser.
First of all the physical symmetry of the two lasers used is not the same. The VCSELs are a vertical emission device while the DFB lasers emit in the horizontal direction. This asymmetry renders the integration of an optical injection-locking system consisting of a DFB laser and a VCSEL very difficult. The second reason, of course, is the cost. One of the reasons of employing VCSELs in optical networks for high-speed data communication is their cost-effectiveness. Utilization of a DFB laser to improve the transmission and the component characteristics compromises this very objective. Due to these reasons despite all these advances regarding this very potent combination of semiconductor lasers and optical injection-locking, the phenomenon and its practical applications have not got any commercial breakthrough as yet.
With the arrival of Vertical-Cavity Surface-Emitting Lasers (VCSELs) on the commercial scene as low-cost, integrable sources, the efforts to revive the optical injection-locking phenomena were once again undertaken and follower VCSEL resonance frequencies ranging from 27 Ghz to 107 GHz have been reported in recent years (Chrostowski et al. 2007). The problem of non-integrability however is still unresolved due to the utilization of a distributed feedback (DFB) laser as master optical source to injection-lock a follower VCSEL. The DFB lasers have horizontal optical cavities. This physical asymmetry renders the monolithic integration very complicated. On the other hand the utilization of a powerful DFB laser compromises the economy of the setup by increasing the cost dramatically and fails the purpose of using a VCSEL in the first place. Clearly the solution to afore-mentioned problems would be to try a VCSEL-by-VCSEL optical injection-locking approach.

3. VCSEL rate equations

The previous chapter introduced the overall historical background of the subject and the motivation for undertaking this research work. In this chapter we will present a complete theoretical analysis of the optical injection-locking phenomenon in semiconductor lasers. A semiconductor laser cavity is essentially a resonator and its input (electrons) and output (photons) can be demonstrated to be interrelated to each other via cavity parameters. Like any other resonator cavity, the quality factor "Q" and the resonance frequency of this cavity can be controlled by manipulating its physical dimensions or intrinsic parameters.
Ordinarily, the only externally manipulable variable is the electron concentration that can be varied by changing the bias current. During the optical injection-locking process the internal parameters of the cavity are changed by varying the photon concentration inside the cavity. Since the locking effect is the result of interaction between two optical fields, the phase difference between the master and follower VCSELs can also be varied to achieve the desired effect.
Ordinarily, the only externally manipulable variable is the electron concentration that can be varied by changing the bias current. During the optical injection-locking process the internal parameters of the cavity are changed by varying the photon concentration inside the cavity. Since the locking effect is the result of interaction between two optical fields, the phase

difference between the master and follower VCSELs can also be varied to achieve the desired effect.

$$\frac{dN(t)}{dt} = \frac{\eta_i I}{qV_{act}} - (A + BN(t) + CN(t)^2)N(t) - v_g GS(t) \quad (1)$$

$$\frac{dS(t)}{dt} = \Gamma\beta BN(t)^2 + \Gamma v_g GS(t) - \frac{S(t)}{\tau_P} \quad (2)$$

Where N(t) and S(t) are the electron and photon densities, η_i the internal quantum efficiency, q the electron charge, V_{act} the active region volume, v_g the group velocity, β the spontaneous emission coefficient, Γ the confinement factor and τ_P the photon lifetime.
The spontaneous emission rate, R_{sp} is defined in terms of the constants A, B and C where A represents the Shockly-Read-Hall non-radiative recombination coefficient, B the bimolecular recombination coefficient and C the Auger non-radiative recombination coefficient. The gain G can be expressed as

$$G = a_0 \frac{N(t) - N_{tr}}{1 + \epsilon S(t)} \quad (3)$$

Where N_{tr} is the transparency carrier density, a_0 the differential gain coefficient and ε the gain compression factor.
A third equation describing the phase behaviour of the device can be introduced as follows:

$$\frac{d\phi(t)}{dt} = \frac{\alpha_H \Gamma v_g a_0}{2}(N(t) - N_{tr}) \quad (4)$$

α_H is the "Phase-Amplitude" coupling factor and is referred to as "Henry's Factor". It might be important to note here that equation 2.4 is not a coupled equation i.e. the term does not appear in equations 2.1 and 2.2. Lang proposed the utilization of three equations, instead of two, to model an optically injection-locked system (Lang, 1982). Lang's equations coupled the electric field variations in the cavity directly to carrier and phase variations and as such rendered the physical interpretation of the phenomenon somewhat cumbersome. In 1985, P. Gallion et al. presented the optical injection-locking rate equations that replaced cavity electrical field by photon number (Gallion & Debarge, 1985), (Gallion et al., 1985). Following the injection of optical power in the optical cavity, the dynamics of the follower laser change. This change can be mathematically presented by modifying the VCSEL rate equations to compensate for optical injection.

$$\frac{dN(t)}{dt} = \frac{\eta I}{qV_{act}} - (A + BN(t) + CN(t)^2)N(t) - v_g GS(t) \quad (5)$$

$$\frac{dS(t)}{dt} = \Gamma v_g GS(t) - \frac{S(t)}{\tau_P} + \frac{v_g}{L}\sqrt{S(t)S_{inj}}\cos(\theta) + \Gamma B\beta N(t)^2 \quad (6)$$

$$\frac{d\phi(t)}{dt} = \frac{\alpha_H \Gamma v_g a_0}{2}(N(t) - N_{tr}) - \Delta\omega - \frac{v_g}{2L}\sqrt{\frac{S_{inj}}{S(t)}}\sin(\theta) \quad (7)$$

It must be remarked that while the equation concerning the carrier density remains unchanged, the equations regarding the phase and the photon density are modified to accommodate for the effects of external light injection.

Two very important parameters of note, S_{inj} and θ are added to equations 2.6 and 2.7. S_{inj} represents the photon density injected inside the follower VCSEL optical cavity while θ denotes the phase difference between the master and follower optical fields so that:

$$\theta = \phi_{inj} - \phi(t) \tag{8}$$

$$\Delta\omega = \omega_{Master} - \omega_{Follower} \tag{9}$$

Apart from frequency detuning, phase difference and injected optical power, the fourth parameter which characterizes an optically injection-locked system is the "coupling coefficient" of a laser. It is defined as k_c and can be expressed mathematically as

$$k_c = \frac{v_g}{2L} \tag{10}$$

This coefficient describes the rate at which the injected electric field adds to the follower cavity electric field as a function of the VCSEL optical cavity length. 'L' is the length of the VCSEL optical cavity.

2.2 Locking Range Calculations

Solving equations (5) and (6) in the steady-state regime which renders $\frac{dS}{sT}$ and $\frac{dN}{sT}$ equal to zero gives the very important parametric equation:

$$\Delta\omega = k_c\sqrt{\frac{S_{inj}}{S}}\left[sin(\theta) - \alpha_H cos(\theta)\right] \tag{11}$$

The dependence of equation (11) on α_H can be elaborated by using the linear combination property for sinuses and cosines. Using this property we can write that:

$$\Delta\omega = k_c\sqrt{\frac{S_{inj}}{S}}\left[\sqrt{1+\alpha_H^2}\right] sin(\theta - \tan^{-1}\alpha_H) \tag{12}$$

This relation is important because it helps the calculation of effective locking bandwidth of an injection-locked system. Moreover it can be deduced that due to the presence of the sine function, the inequality is limited to the range of:

$$|\Delta\omega| \leq k_c\sqrt{\frac{S_{inj}}{S}}\left[\sqrt{1+\alpha_H^2}\right] \tag{13}$$

On the other hand, it appears that the oscillation limit for θ is between $-\pi/2$ and $\pi/2$. $\Delta\omega$ is then bounded by:

$$-k_c\sqrt{\frac{S_{inj}}{S}}\left[\sqrt{1+\alpha_H^2}\right] \leq \Delta\omega \leq k_c\sqrt{\frac{S_{inj}}{S}} \tag{14}$$

The asymmetry of the locking range can be explained both mathematically and physically. Mathematically speaking, if we observe (14), we can see that due to the multiplication with the term α_H on the left hand side, this relation becomes asymmetric with respect to α_H.

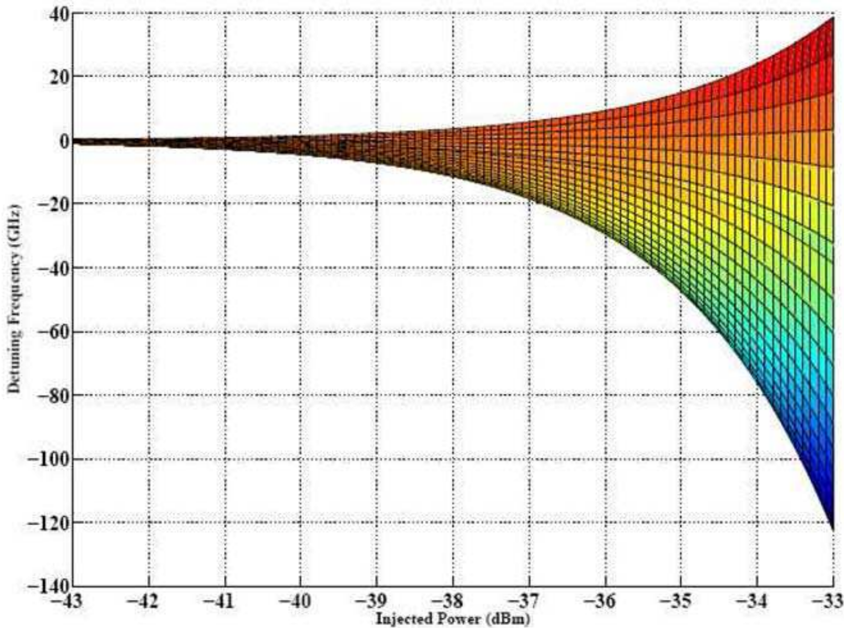

Fig. 7. 2D presentation of calculated locking range of a long wavelength VCSEL with $\alpha_H = 3$ showing the locking-range dependence on injected optical power.

Physically speaking, during the injection-locking of a semiconductor laser the increased photon population changes the refractive index and leads to a cavity wavelength shift in the longer wavelength direction and finally an asymmetric locking range. Calculated locking-range for $\alpha_H = 3$ is presented in fig. 7. It can be observed from equation (14) that a higher value of α_H leads to higher locking-range: A higher value of α_H favours locking in the negative frequency detuning range. In terms of locking-range characteristics, VCSELs are different from EELs. Locking range determines the extent of frequency enhancement of an optically injection-locked laser. Equation (14) shows that the locking-range depends on injected power and coupling coefficient k_c. Therefore mathematically it can be stated that the locking-range follows the variation of the term $k_c \sqrt{S_{inj}/S}$.

Since a VCSEL cavity is much shorter than an EEL cavity, VCSELs have typically very high values of k_c (10) as compared to those of conventional lasers. This implies that VCSEL locking-ranges are higher compared to EEL locking-ranges and can potentially lead to much higher resonance frequencies.

3.1 Small signal analysis

We begin by presenting once again the "Modified VCSEL Rate Equations". The small signal analysis is performed to derive the S_{21} response of an injection-locked VCSEL. Consider that a sinusoidal signal modulates a laser biased at current I. The resulting expression for current I then becomes:

$$I(t) = \bar{I} + \Delta I e^{j\omega t} \tag{15}$$

Similarly, the carrier, photon and phase variations can be described as follows:

$$N(t) = \overline{N} + \Delta N e^{j\omega t} \tag{16}$$

$$S(t) = \overline{S} + \Delta S e^{j\omega t} \tag{17}$$

$$\phi(t) = \overline{\phi} + \Delta \phi e^{j\omega t} \tag{18}$$

By putting

$$\dot{N} = \frac{dN}{dt} \tag{19}$$

$$\dot{S} = \frac{dS}{dt} \tag{20}$$

$$\dot{\phi} = \frac{d\phi}{dt} \tag{21}$$

We have:

$$\Delta\dot{N}(I,N,S) = \frac{\partial \dot{N}}{\partial I}\cdot\Delta I + \frac{\partial \dot{N}}{\partial N}\cdot\Delta N + \frac{\partial \dot{N}}{\partial S}\cdot\Delta S \tag{22}$$

$$\Delta\dot{S}(N,S,\phi) = \frac{\partial \dot{S}}{\partial N}\cdot\Delta N + \frac{\partial \dot{S}}{\partial S}\cdot\Delta S + \frac{\partial \dot{N}}{\partial \phi}\cdot\Delta \phi \tag{23}$$

$$\Delta\dot{\phi}(N,S,\phi) = \frac{\partial \dot{\phi}}{\partial N}\cdot\Delta N + \frac{\partial \dot{\phi}}{\partial S}\cdot\Delta S + \frac{\partial \dot{\phi}}{\partial \phi}\cdot\Delta \phi \tag{24}$$

The gain, as defined in (3), contains both the carrier and the photon terms. Partial differentiation of (3), with respect to the carrier and photon densities N and S, yields two new variables G_N and G_S, where G_N and G_S are defined as:

$$G_N = \frac{\partial G}{\partial N} = \frac{a_0}{1+\epsilon S} \tag{25}$$

$$G_S = -\frac{\partial G}{\partial S} = \frac{a_0\epsilon(N-N_{tr})}{(1+\epsilon S)^2} \tag{26}$$

Differentiating equation (5) with respect to N, S and ϕ therefore results in the following set of three equations:

$$\frac{\partial \dot{N}}{\partial N}\cdot\Delta N = (-(A+2BN+3CN^2) - v_g G_N S)\Delta N \tag{27}$$

$$\frac{\partial \dot{N}}{\partial S}\cdot\Delta S = (-v_g G + v_g G_S S)\Delta S \tag{28}$$

$$\frac{\partial \dot{N}}{\partial I}\cdot\Delta I = \frac{\eta_i}{qV_{act}}\Delta I \tag{29}$$

Thank You for previewing this eBook

You can read the full version of this eBook in different formats:

- HTML (Free /Available to everyone)
- PDF / TXT (Available to V.I.P. members. Free Standard members can access up to 5 PDF/TXT eBooks per month each month)
- Epub & Mobipocket (Exclusive to V.I.P. members)

To download this full book, simply select the format you desire below